LA-UR -82-2833

CONF-820865--2

Los Alamos National Laboratory is operated by the University of California for the United States Department of Energy under contract W-7405-ENG-36.

MASTER

LA-UR--82-2833

DE83 000604

TITLE: NATURAL-GAS-HYDRATE DEPOSITS: A REVIEW OF IN-SITU PROPERTIES

AUTHOR(S): P. M. Halleck, C. Pearson, P. L. McGuire, R. Hermes, and M. Mathews

SUBMITTED TO: Proceedings, Conference of Physics and Chemistry of Ice
Rolla, Missouri
August 1982

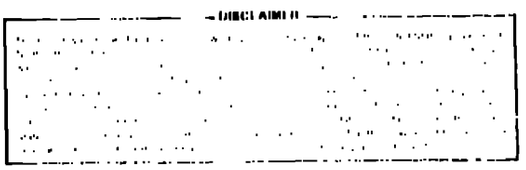

Los Alamos Los Alamos National Laboratory
Los Alamos, New Mexico 87545

NATURAL GAS HYDRATE DEPOSITS:

A REVIEW OF IN SITU PROPERTIES

P. M. Halleck, C. Pearson,
P. L. McGuire, R. Hermes, and M. Mathews
Los Alamos National Laboratory
Geophysics Group, MS C335
Los Alamos, New Mexico 87545

ABSTRACT

Hydrates of natural gas exist in nature in the Arctic regions and underneath the sea floor. If the trapped gases can be released, they are a huge potential energy resource with worldwide reservoir estimates ranging as high as 10^7 trillion cu ft (TCF). The Los Alamos hydrate project has concentrated on three activities. First, we have evaluated techniques to produce gas from hydrate deposits to determine critical reservoir and production variables. Second, we have predicted physical properties of hydrate-containing sediments both for their effects on production models and to allow us to develop geophysical exploration and reservoir characterization techniques. Third, we are measuring properties of synthetic hydrate cores in the laboratory.

Exploration techniques can help assess the size of potential hydrate deposits and determine which production techniques are appropriate for particular deposits. Unfortunately, so little is known about the physical properties of hydrate deposits that it is difficult to develop geophysical techniques to locate or characterize them. However, because of the strong similarity between hydrates and ice, empirical relationships between ice composition and seismic velocity, electrical resistivity, density, and heat capacity that have been established for frozen rocks may be used to estimate the physical properties of hydrate deposits.

The resistivities of laboratory permafrost samples are shown to follow a variation of Archie's equation,

$$\frac{\rho_t}{\rho_f} = C^{-T} Sw^{1-n} \quad ,$$

where ρ_t and ρ_f are the thawed and frozen resistivities of the sample, T is temperature, Sw is the unfrozen water content, and n and C are empirical constants. Using multiple linear regression techniques, we calculate C and n for a variety of lithologic types.

The compressional wave velocities of partially frozen sediments (V_p) are related to the velocity of the matrix (V_m) and to the liquid (V_l) and solids (V_s) phases present in the pores by the well-known three-phase rule:

$$\frac{1}{V_p} = \frac{\phi(Sw)}{V_l} + \frac{\phi(1 - Sw)}{V_s} + \frac{(1 - \phi)}{V_m} \quad ,$$

where ϕ is the porosity. Clearly, both the resistivities and seismic velocities are functions of the unfrozen water content; however, resistivities are more sensitive to changes in Sw, varying by as much as three orders of magnitude, which may allow the use of electrical resistivity measurements to estimate the amount of hydrate in place.

We estimated the unfrozen water content, assuming that the dissolved salt in the pore water is concentrated as a brine phase as the hydrates form. Using this technique, we estimated the brine content as a function of depth, assuming several temperature gradients and pore water salinities. We find

that hydrate-bearing zones are characterized by high seismic velocities and electrical resistivities compared to unfrozen sediments or permafrost zones.

Surprisingly, hydrates may also have higher resistivities than permafrost deposits, due to lower amounts of unfrozen water contained by the hydrate deposits. The presence of hydrates also tends to lower the heat capacities and densities of sediments, but these effects are comparatively small and not useful for exploration.

INTRODUCTION

Hydrates of methane and other constituents of natural gas, which have been known for years as a laboratory curiosity and an occasional problem in gas transmission lines, have only recently been discovered in nature (Chersky and Makogon 1970). Gas hydrate reserves are restricted to permafrost regions in the Arctic on land and to the continental slopes and rises offshore. While naturally occurring methane hydrate deposits are new to science, they are fairly widespread in nature (Chersky and Mahogon 1970) with some estimates of the worldwide reservoir ranging as high as $1.5 \times 10^{18} m^3$ (Barraclough 1980), enough to stimulate interest in hydrates as a possible energy source.

Unfortunately, very little is known about the physical properties of natural gas hydrate deposits in nature making their detection by remote geophysical surveys very difficult. In this paper we review experimental sonic and resistivity measurements on hydrates, hydrate-bearing sediment, and permafrost. We conclude that hydrate layers are characterized by anomolously high sonic velocities and resistivities, both of which are functions of the amount of liquid water associated with the hydrates in the rock matrix. Using an analogy between hydrate-bearing sediments and permafrost, we propose simple quantitative relationships between liquid water content and the electrical

resistivities and sonic velocities of the deposits. Finally we present electrical and sonic well logging data that substantiates the basic conclusions of this paper.

RESISTIVITIES

There are no reported laboratory resistivity measurements on hydrate-containing sediments, however there is an extensive body of literature on the electrical properties of partly frozen sediments. Ice is an electrical insulator. Because ice and hydrates have a similar crystal structure, hydrates probably are electrical insulators also. Thus, the resistivities of permafrost and hydrate deposits are largely controlled by unfrozen brine inclusions.

Archie's law (Archie 1942), ($\rho = a\ \rho_w\ \emptyset^{-m}\ Sw^{-n}$), is an empirical relationship between water content and the resistivity of water-saturated sediments. Here ρ is the resistivity of the sediments, ρ_w is the pore water resistivity, Sw is the fraction of the porosity occupied by liquid water, and a, m, and n are empirically derived parameters. This equation also applies to rocks where the pore spaces are partially filled with ice of hydrates. However, as the amount of liquid water decreases, Sw and ρ_w are both reduced, Sw because some of the available pore space is now filled with a solid nonconductor, and ρ_w because the dissolved salts are concentrated in the remaining unfrozen water. If the brine is not very near saturation, the effect of hydrate or ice formation on ρ_w is relatively easy to quantify because an increase in salt concentration causes a linear decrease in ρ_w. Because hydrates and ice exclude all of the dissolved salts as they form, the salt concentration of the brine inclusions is inversely proportional to the volume fraction of liquid water, assuming that the sediments were initially water-saturated. In

addition, the resistivity of aqueous solutions increases exponentially with decreasing temperatures. Including both the temperature and concentration effects, the resistivity of a partially frozen brine at temperature T is thus proportional to $(C)^T$ Sw where C is a constant. Substituting this relationship into Archie's equation and dividing by the resistivity at 0°C, we find that the ratio of frozen (ρ_f) and thawed (ρ_t) resistivities is

$$\rho_f/\rho_t = C^{-T}\, Sw^{1-n} \quad . \tag{1}$$

ESTIMATING THE EMPIRICAL CONSTANTS IN ARCHIE'S EQUATION

To use this relationship, the empirical constants C and n must be known. Fortunately, Pandit and King (1979), Hoyer et al. (1975), Desai and Moore (1967), and Dumas (1962) have all examined the relationship between formation temperatures, pore water resistivities, and formation resistivities. In all four studies, rock or soil samples, ranging in composition from sandstones and limestones to fine sands and silts, were saturated with dilute brines with known composition. Resistivities of these samples were then measured repeatedly as the temperature was varied from above the freezing point to -21.1°C, the eutetic of the water NaCl system. Because the samples were saturated with saline water, the pore water did not completely freeze when the temperature was decreased below the freezing point. As ice formed in the pores, the dissolved salts concentrate in the remaining liquid or brine phase. However, ice can only form until the brine concentration reaches a critical value where the freezing point of the brine equals the temperature. Using the well-known freezing point depression curves for the water NaCl system, we estimated the concentration of the brine phase and the amount of unfrozen water present in the sample. We then used this data to test Eq. (1) and estimate the value of n and C, the empirical constants.

Clearly this technique assumes that the salinity measured outside the rock is equal to the in situ salinity. Unfortunately, interactions between pore water and grain surfaces can cause exchangeable ions contained in the rock matrix to go into solution, forming an ion halo around each grain boundary. However, these extra ions have an important effect on the water resistivities only if the dissolved ion concentration is initially quite low. In addition, surface chemistry effects can cause pore water to freeze at temperatures below those calculated from the freezing point depression curves. However, Patterson and Smith (1981) show that, for soil samples containing silt and sand, surface chemistry effects depress the freezing point by less than one degree, although the effect can be considerably greater if significant amounts of clay are present.

We estimated the empirical parameters C and n using multivariate linear regression techniques. In order to estimate n and C using linear regression, we inverted Eq. (2) and took the log of both sides.

$$\log (\rho_t/\rho_t) = T \log (C) + (n - 1) \log (Sw) \quad . \tag{2}$$

Our dependent variable was thus log (ρ_t/ρ_f) and the first two independent variables were T and log (Sw). Using this simple regression model, we found that n is equal to 2.01 and C is equal to 1.05.

To examine the effects of lithology, we expanded this simple model using qualitative or indicator variables Indicator variables can take on one of two values, depending on whether or not the sample is a member of a particular qualitative class. We used two qualitative variables in the expanded model to test the effect of lithology. The first compared consolidated and unconsolidated sediments, and the second compared limestones with sands and sandstones.

We also included cross products between the two qualitative variables and log (Sw) because this allowed us to independently estimate n for the three lithologic classes. Values of the empirical parameters calculated from this regression model are listed in Table I. Figure 1 illustrates the scatter of the data about the regression model.

FREQUENCY DEPENDENCE

The frequency dependence of the resistivities is an important topic because field resistivity measurements are made over a broad frequency range from 0-30,000 Hz (Hoekstra 1974). Olhoeft (1975, 1977) examined the frequency dependence of resistivity for partially frozen soils. Olhoeft concludes that at low frequencies (below 10-1000 Hz) ionic conduction in the brine phase controls the resistivitiy. At frequencies above 1 kHz, the resistivity appears to decrease with increasing frequency as a result of migration of Bjerrum defects (Runnels 1969), which reduces the resistivity of ice at these frequencies.

In the absence of clays, the resistivity is nearly frequency independent to frequencies in excess of 1 kHz (Pandit and King 1978). However, if the sample contains much clay, a strong frequency dependence can start at frequencies as low as 10-100 Hz. Olhoeft (1977) ascribes this frequency to charged layers surrounding conductors embedded in a dielectric medium, that is, the Maxwell Wagner effect (Hasted 1973). Because clay minerals have a much higher surface area to volume ratio this mechanism may only be important if clay is present in the sample. Although all these measurements have been made in permafrost samples, hydrates have a similar structure and the same mechanisms may also be important in hydrate-bearing sediments. The frequency

dependent resistivity of hydrates is likely to be somewhat more complex, especially at high frequencies because of the effect of the guest molecules.

SONIC VELOCITIES

The most accurate estimates of the sonic velocities of natural gas hydrates thus far are calculated compressional velocities published by Whalley (1980). Following that approach, the compressional wave velocity (V_p) is related to the adiabatic Young's modulus E and Poission's ratio ν by

$$Vp^2 = E \frac{(1 - \nu)}{\rho(1 + \nu)(1 - 2\nu)} \quad , \tag{3}$$

where ρ is the density (Landau and Lifschitz 1963). However, $\kappa_S = (1-2\nu)/E$ and $\kappa_S/\kappa_T = 1 - \alpha^2 TV/\kappa_T C_p)$ where α is the volume thermal expansivity, κ_S and κ_T are the adiabatic and isothermal compressibilities, T is temperature, V is molar volume, and C_p is the heat capacity at constant pressure. Substituting into Eq. (2),

$$Vp^2 = \frac{(1 - \nu)}{(1 - \nu)\,\rho\,\left(1 - \frac{\alpha^2 TV}{\kappa_T C_p}\right)\,\kappa_T} \quad . \tag{4}$$

The ratio of the compressional wave velocities of ice (Vpi) and hydrates (Vph), is just the ratio of Eq. (3) evaluated for ice and hydrates respectively:

$$\frac{Vp_h^2}{Vp_i} = \frac{\kappa_T\,\rho_i\,(1 - \nu_h)(1 + \nu_i)\left(1 - \frac{\alpha_i\,TV_i}{\kappa_{Ti}\,C_{pi}}\right)}{Th\,\rho_h\,(1 - \nu_i)(1 + \nu_h)\left(1 - \frac{\alpha_h\,TV_h}{\kappa_{Th}\,C_{ph}}\right)} \quad . \tag{5}$$

Following Whalley, we assume that Poisson's ratio and the volume thermal expansivity are equal in hydrates and ice. The isothermal compressibility

(κ_T) of hydrates has not been measured; however, we can estimate it using the following formula

$$\kappa_T = \frac{9}{NK_2r^2} \quad , \tag{6}$$

where N is the number of bonds between water molecules, r is the mean bond length, and K_2 is the harmonic force constant of the bond. Because all these quantities can be estimated from spectral or x-ray diffraction data, we can use Eq. (5) to estimate κ_T. Because the interactions between the guest molecules and the lattice are much weaker than the bonds between the water molecules in the lattice, κ_T does not depend significantly on the guest molecule or the occupancy ratio.

The heat capacity of ice is about 37.7 J/K mol, and this is probably about equal to the heat capacity of empty hydrate lattice. However, the heat capacity of hydrates is strongly influenced by the guest molecule. Because the guest molecule in the case of methane can rotate freely and vibrate against the crystal lattice, it has a rotational heat capacity of 3/2 R and a vibrational heat capacity of 3 R. In addition, intermolecular vibrations will occur and these contribute nR to the heat capacity where n is the number of bonds in the guest molecule. So the total heat capacity of the hydrate is 37 + (9+2n)/2 RL where L is the number of mols of guest/mol of water, and n depends on the guest. Table II lists typical compressional wave velocities for hydrates. Note that Vp can vary 19% depending on composition and occupancy ratio.

Seismic velocities of propane and hydrate methane have been measured by Pandit and King (1981) and Whiffen et al. (1982). Pandit and King measured compressional wave velocities of a maximum of 3.2 km/s, or only 84% of ice for propane hydrate, much lower than the Whalley model would predict. The reasons

for this discrepancy are not clear, however, the densities of the hydrate samples used by Pandit and King are 750 kg/m^3, only 80% of the values calculated by Whalley (1980). This may imply that the samples contained liquid propane inclusions. Wiffen et al. measured the sonic velocity of methane hydrate using Brillouin Spectroscopy. They measured a compressional wave velocity of approximately 91% the velocity of ice. This measurement is in agreement with Whalley's calculations.

The compressional velocity of a mixture of ice and unfrozen brine in the interstitial pore species of a rock can be estimated using a three-phase time-averaged equation, first proposed by Timur (1968) and since tested by several other authors. The compressional velocity (Vp) is related to the velocity of ice (Vs), the velocity of the brine inclusions (Vb), and the velocity of the solid matrix (Vm) by

$$1/Vp = \frac{\emptyset(1 - Si)}{Vb} + \frac{\emptyset\, Si}{Vs} + \frac{(1 - \emptyset)}{Vm} \quad , \tag{7}$$

where Si is the fraction of ice in the rock. Because of the similarities between the seismic velocities of ice and hydrates, this equation can probably be used to calculate the velocity of a mixture of hydrates and brine in sedimentary rock.

PHYSICAL PROPERTIES OF GAS HYDRATE DEPOSITS AND ICE IN SITU

Natural gas hydrate deposits and permafrost consist of porous sedimentary rock whose pore spaces are partially or completely filled with hydrates or ice. The physical properties of these deposits thus depend on the properties of the rock matrix, the hydrates, and the amount and composition of the unfrozen water or gas that also may be present in the pores. A liquid water phase will nearly always be present because of ions dissolved in the pore

waters. We calculate Sw for hydrate solutions by plotting the pressures and temperatures associated with points along the geothermal gradient on a family of hydrate stability curves for different NaCl solutions (after Kobayashi et al. 1951) and then using the curves to estimate brine concentration at equilibrium with methane hydrates. We used a very similar method to estimate the brine concentrations in permafrost. Once we calculate the brine phase concentrations, we can easily calculate Sw assuming that none of the dissolved ions diffuse out of the partially frozen sediments. Once Sw as a function of depth is known, we can calculate the resistivities and sonic velocities using Eqs. (1 and 6). The calculation is shown graphically in Figs. 2 and 3. Note that hydrate-bearing sediments have resistivity higher than both thawed sediments (ρf = 10 Ω-m) and permafrost. A similar calculation for marine deposits is shown in Figs. 4 and 5. Sonic velocities also increase when hydrates are present however proportionately, the increase is much smaller than is the case with resistivities. Also while sonic velocities are not as strongly dependent on the unfrozen water content as the electrical resistivity and thus have a relatively constant high value if hydrates are present. This effect is potentially important because high sonic velocities are thus a qualitative indicator of the presence of hydrates while electrical resistivities quantitatively indicate the amount of hydrates in place.

WELL LOGGING DATA

The limited amount of well logging data available tends to qualitatively support our model of the physical properties of hydrate-bearing sediments. Figure 6 shows sonic and resistivity logs from known hydrate-bearing formations. Clearly hydrates are characterized by high sonic velocities and

resistivities compared to unhydrated sediments and the proportional increase in sonic velocity is less than the electrical resistivity.

CONCLUSION

Very little published data exist on the physical properties of natural gas hydrates. However, because of the strong similarity between hydrates and ice, empirical relationships originally developed for permafrost are used to estimate the physical properties of hydrate deposits. Three major conclusions are drawn from this study.

(1) Hydrate deposits will have much higher resistivities and sonic velocities than similar unfrozen sediments. Hydrates will also tend to reduce the thermal conductivities and densities of sediments, but these effects are comparatively small (usually less than 5%) (Pearson 1982) so seismic and electrical methods will be the most useful geophysical techniques when exploring for hydrate deposits.

(2) Surprisingly, hydrate deposits that form above the 0°C isotherm will often have higher resistivities than nearby permafrost deposits. This is because hydrate deposits, which form near the bottom of the permafrost zone, usually contain smaller amounts of unfrozen water than permafrost. This characteristic may be useful in distinguishing ice and permafrost.

(3) All of the physical properties of hydrate deposits are functions of the unfrozen water content. This is particularly true of the electrical resistivity that can vary as much as three orders of magnitude. This effect is potentially very useful because it may be possible to calculate the unfrozen water content in hydrate deposits from geophysical measurements.

(4) Of the physical properties examined in this report, sonic velocities and resistivities are the most strongly affected by the presence of hydrates. However, unlike resistivities, sonic velocities are not strongly affected by the amount of unfrozen water present. Thus, high sonic velocities provide a qualitative indication of the presence of hydrates whereas resistivities provide a quantitative indication of the amount of hydrate present. Clearly both measurements are potentially valuable in evaluating hydrate deposits.

Because the resistivities of natural gas hydrate-bearing sediments are strongly affected by the amount of free water present in the deposit, resistivity measurements may be very useful in evaluating hydrate deposits and determining what production methods have the best chance of producing the natural gas. McGuire (1981) proposes two methods of producing natural gas from hydrate deposits. In the first method, warm water injected into a hydrate deposit dissociates the hydrates and the resulting free gas is recovered from nearby production wells. Unfortunately in order to work, this method requires quite high permeabilities. In a second method (which may produce natural hydrate deposits) reduction of pore pressure causes the hydrates to disassociate. Because the low permeabilities of hydrate-bearing deposits are caused by hydrates clogging the pore spaces, hydrates with low resistivities, and a high unfrozen water content, may have relatively high permeabilities and thus are candidates for the first production method whereas hydrate deposits with high resistivity may be candidates for the second method.

REFERENCES

Archie, C. E., The electrical resistivity log as an aid in determining some reservoir characteristics, Trans. AIME 146, pp. 54-62, 1942.

Barraclough, B. L., Methane hydrates as an energy resource: a review with recommendations for future research, Los Alamos National Laboratory report LA-8368-MS (June 1980).

Chersky, N. and Y. Makogon, Solid gas - world reserves are enormous, Oil Gas Invest., v. 10, p. 82, 1970.

Davidson, D. W., Clathrate hydrates in water, a comprehensive treatise, v. 2, F. Franks, Ed., pp. 115-234, Plenum, New York, 1973.

Desai, K. P. and E. J. Moore, Well log interpretation in permafrost, Trans. Soc. Prof. Well Log Analysts, pp. 1-27, 1967.

Dumas, M. C., Electrical resistivities and dielectric constants of frozen rocks, M.S. thesis, Colorado School of Mines, Golden, Colorado, 1962.

Hasted, J. B., Aqueous Dielectrics, Chapman and Hall, London, 1973.

Hoekstra, P. and A. Delaney, Dielectric properties of soils at UHF and Microwave frequencies, J. Geophys. Res., 79, 1699-1708, 1974.

Hoyer, W. A., S. O. Simmons, M. M. Spann, and A. T. Watson, Evaluation of permafrost with well logs, Trans. Soc. Proc. Well Log Analysts pp. 1-15, 1975.

Kobayashi, R., H. J. Withrow, G. B. Williams, and D. L. Katz, Gas hydrate formation with brine and ethanal solutions, Proc., National Gasoline Assoc. Am., pp. 27-31, 1951.

Landau, L. D. and E. M. Lifschitz, Theory of elasticity, Pergamon, New York, 1963.

McGuire, P., Methane hydrate gas production: an assessment of conventional production technology as applied to hydrate gas recovery, Los Alamos National Laboratory report LA-9102-MS (November 1981).

Olhoeft, G. R., Electrical properties of permafrost, PhD thesis, Dept. of Physics, Univ. of Toronto, Toronto, Canada, 1975.

Olhoeft, G. R., Electrical properties of natural clay permafrost, Canada J. Earth Sci. 14, pp. 16-24, 1977.

Pandit, B. I. and M. S. King, Influence of pore water salinity on seismic and electrical properties of rocks at permafrost temperature, Proc. Third Intern. Conf. Permafrost Nat. Res. Coun. Canada, pp. 553-559, 1978.

Pandit, B. I. and M. S. King, A study on the effects of pore water salinity on the physical properties of sedimentary rocks at permafrost temperatures, Canada J. Earth Sci. 16, pp. 1566-1580, 1979.

Pandit, B. I. and M. S. King, Elastic wave propagation in propane gas hydrates, Proc. Fourth Canadian Permafrost Conf., Nat. Res. Coun. of Canada, 1981 (in press).

Patterson, D. E. and M. W. Smith, The measurement of unfrozen water content by time domain reflectometry: results from laboratory tests, Can. Geotech J., 18, pp. 131-144, 1981.

Pearson, C., Physical properties of natural gas hydrate deposits, Los Alamos National Laboratory report LA-9422-MS (June 1982).

Runnels, L. K., Diffusion and relaxation phenomena in ice, pp. 514-526, in Physics of Ice, Riehl, N., B. Bullemer, and H. Engelhardt, Eds., Plenum, New York, 1969.

Stoll, R. D. and G. M. Bryan, Physical properties of sediments containing gas hydrates, J. Geophys. Res., v. 84, pp. 1629-1634, 1979.

Timur, A., Velocity of compressional waves in porous media at permafrost temperatures, Geophysics, v. 33, pp. 584-595, 1968.

Whalley, E., Speed of longitudinal sound in clathrate hydrates, J. Geophys. Res., v. 85, pp. 2539-2542, 1980.

Whiffen, B. L., H. Kiefte, and M. J. Clouter, Determination of acoustic velocities in xenon and methane hydrates by Brillouin Spectroscopy, Geophys. Res. Lett., (in press).

TABLE I

CALCULATION OF EMPIRICAL PARAMETERS

$$\rho_t/\rho_f = a\ Sw^{n-1}\ C^T$$

Lithology	n	c	a	Number of Points
Sandstone	2.24 ± 0.02	1.04 ± 0.01	1.7 ± 0.2	87
Limestone	1.8 ± 0.01	1.04 ± 0.01	1.3 ± 1.2	21
Unconsolidated Material	1.7 ± 0.1	1.04 ± 0.01	0.5 ± 0.3	28
Pooled Estimate	2.01 ± 0.02	1.05 ± 0.01	1.3 ± 0.3	136

All errors calculated to the 95% level of confidence.

TABLE II

VELOCITIES OF GAS HYDRATES

Guest	Vp km/s	
	100% Occupancy	80% Occupancy
C_3H_8	3.92	3.98
CH_3	3.73	3.78
CO_2	3.35	3.46
H_2S	3.47	3.56
C_2H_6	3.80	3.90
$C_3H_8 + CH_3$	3.78	

FIGURE CAPTIONS

Figure 1. Pt/Pf plotted vs Sw for the three lithologic divisions considered in the multiple regression analysis. We have compensated for the effect of temperature in these data. The regression lines have slope n-1 and intercept log (a). The scatter of the data about the lines illustrates the fit to the regression model.

Figure 2. Geothermal gradient for land hydrate deposits plotted on Kobayashi's (1951) curves. Surface temp = -6°C.

Figure 3. Velocities and resistivities vs depth for the geothermal gradients shown in Fig. 4.

Figure 4. Geothermal gradients for ocean bottom hydrate deposit plotted on Kobayashi's (1951) curves. Deposits are at a depth of 1 km. Surface temperature is 2°C.

Figure 5. Velocities and resistivities for the geothermal gradients shown in Fig. 6.

Figure 6. Well logging data from a deep sea drilling program CDSDP well (Mark Mathews, Los Alamos National Laboratory, personal communication).

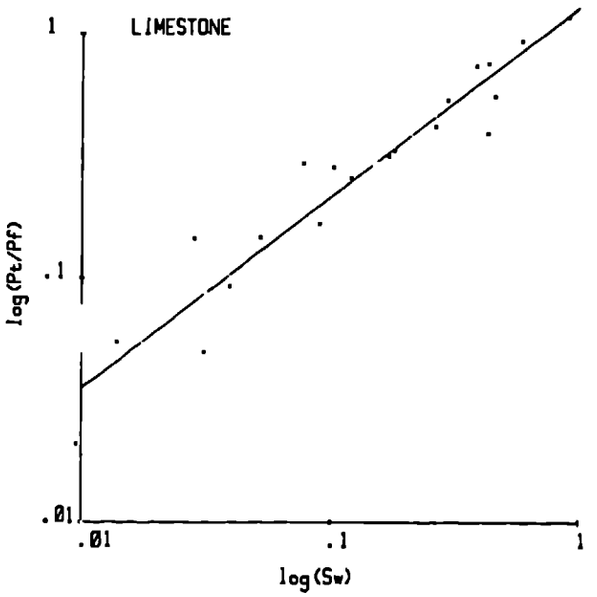
LIMESTONE
1
.1
.01
log (Pt/Pf)
.01
.1
1
log (Sw)

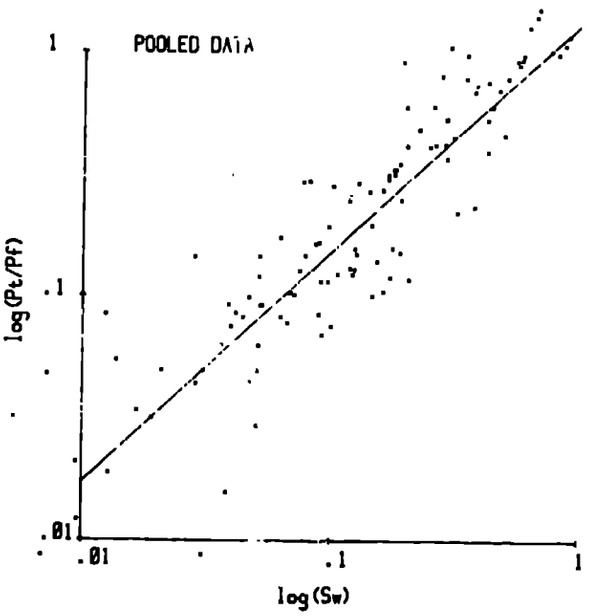
POOLED DATA
1
.1
.01
log (Pt/Pf)
.01
.1
1
log (Sw)

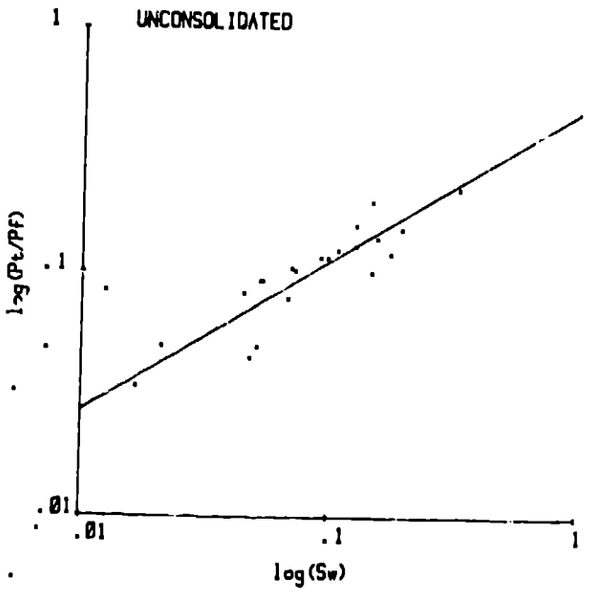
UNCONSOLIDATED
1
.1
.01
log (Pt/Pf)
.01
.1
1
log (Sw)

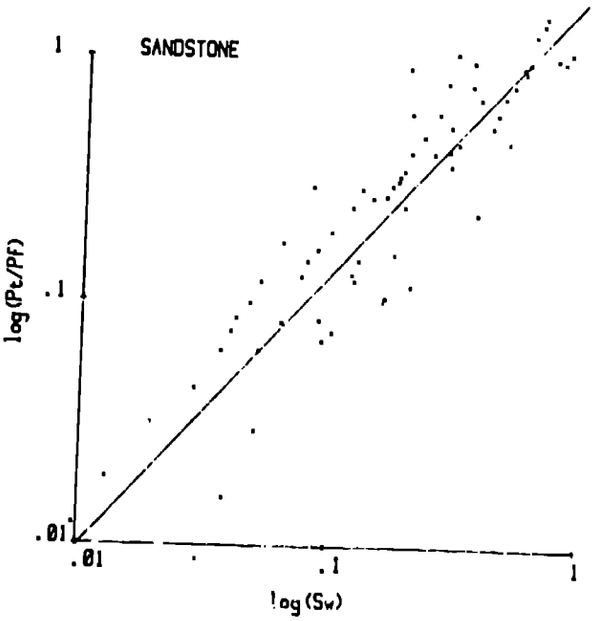
SANDSTONE
1
.1
.01
log (Pt/Pf)
.01
.1
1
log (Sw)

Pressure (MPa)
1
10
-10
0
10
20
Temperature (C)
20
30
40
50
60
Temperature (F)
100
200
400
600
800
1000
2000
4000
Pressure (psi)
21
18
16
14
12
10
7
0
Wt% NaCl
Methane - Pure Water
16°C/km

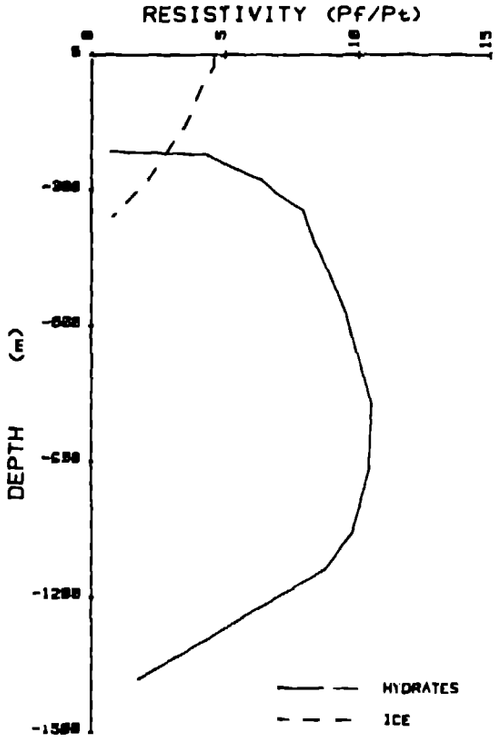
RESISTIVITY (Pf/Pt)
DEPTH (m)
HYDRATES
ICE

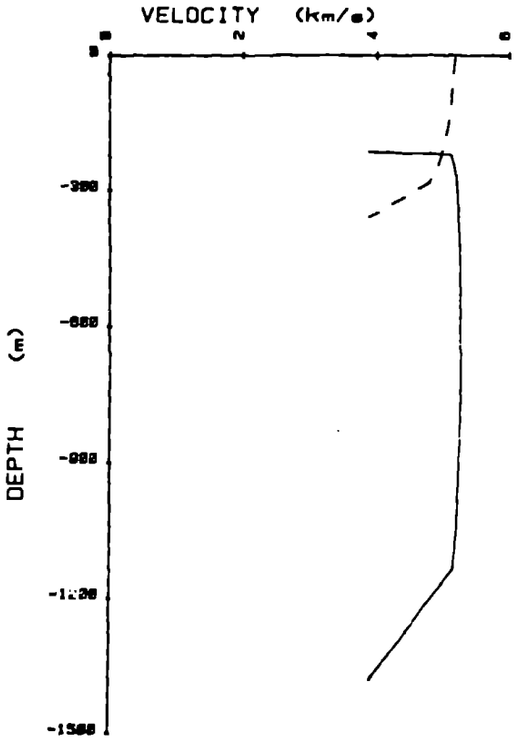
VELOCITY (km/s)
DEPTH (m)

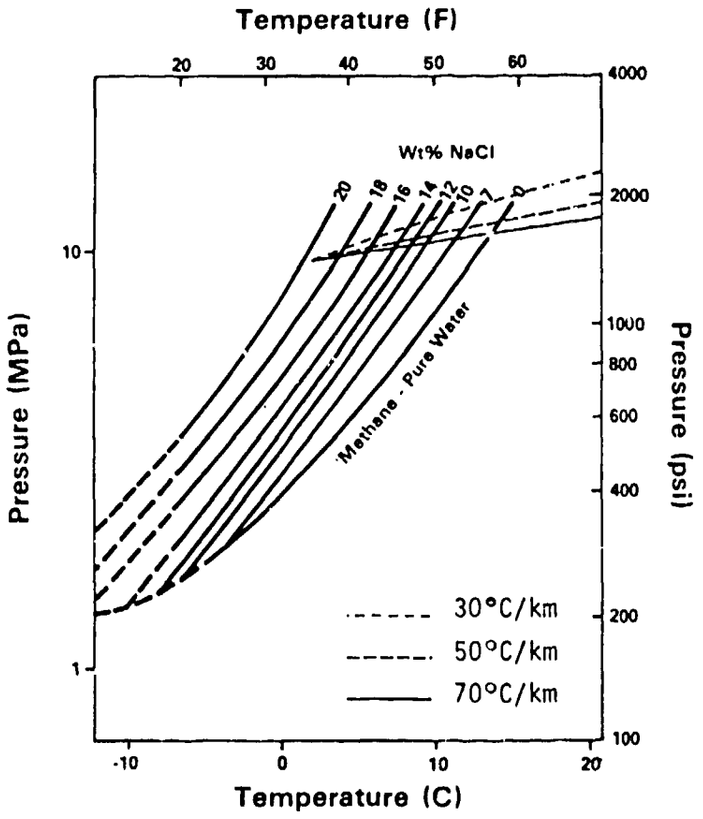
Temperature (F)
20
30
40
50
60
4000
Wt% NaCl
20
18
16
14
12
10
7
0
2000
10
1000
800
600
400
Pressure (MPa)
Pressure (psi)
Methane - Pure Water
30°C/km
50°C/km
70°C/km
200
1
100
-10
0
10
20
Temperature (C)

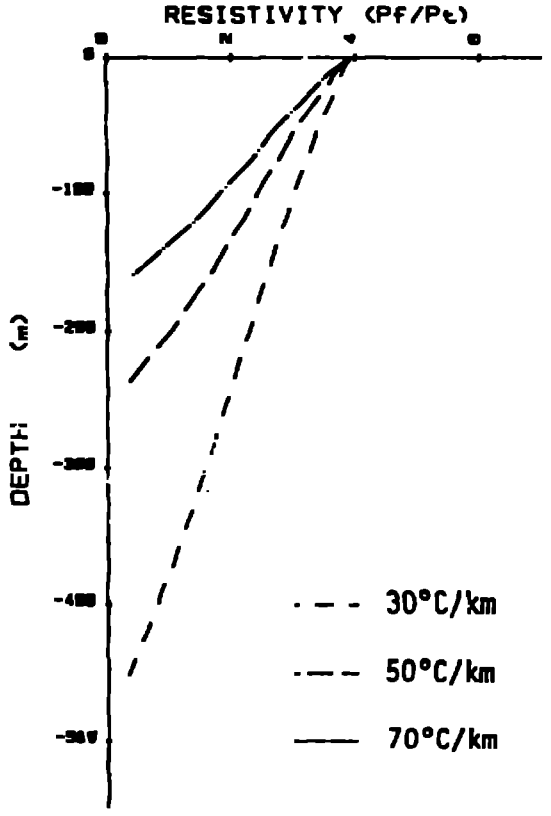
RESISTIVITY (Pf/Pe)
DEPTH (m)
30°C/km
50°C/km
70°C/km

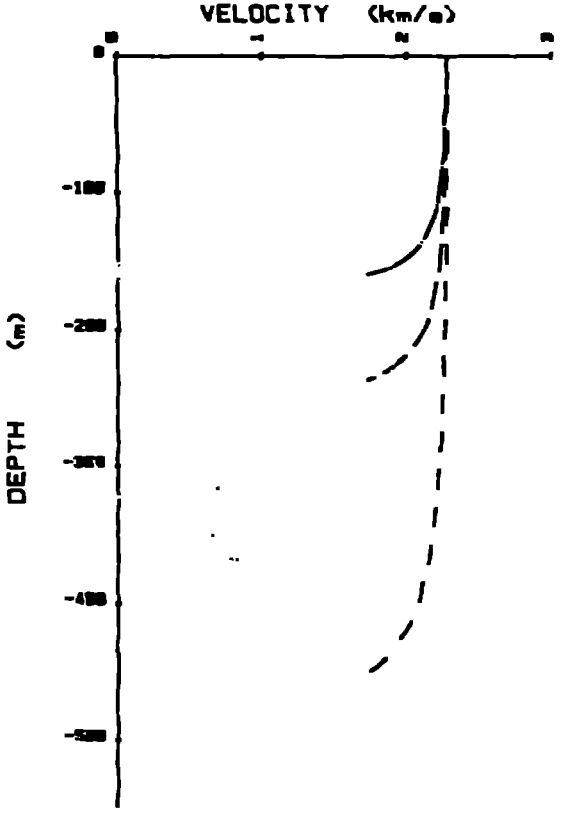
VELOCITY (km/s)
DEPTH (m)

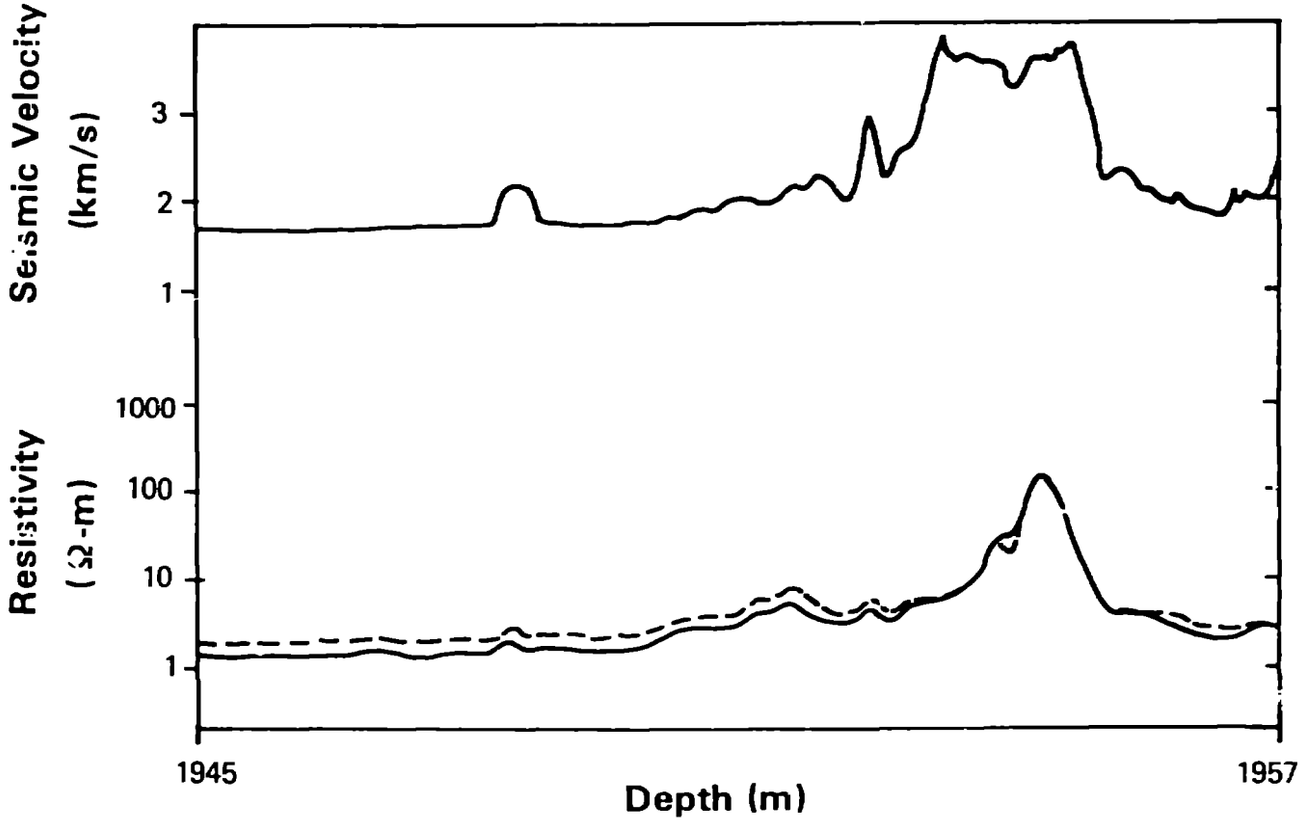
Seismic Velocity
(km/s)
3
2
1
Resistivity
(Ω-m)
1000
100
10
1
1945
1957
Depth (m)